

Fabrication of a Lateral Flow Assay for Rapid In-Field Detection of COVID-19 Antibodies Using Additive Manufacturing Printing Technologies

Abdulelah A. Alrashoudi^{1†}, Hamed I. Albalawi^{1†}, Ali H. Aldoukhi^{1†}, Manola Moretti¹, Panayiotis Bilalis¹, Malak Abedalthagafi^{2,3}, Charlotte A. E. Hauser^{1,4*}

¹Laboratory for Nanomedicine, Division of Biological and Environmental Science and Engineering, King Abdullah University of Science and Technology, Thuwal 23955-6900, Saudi Arabia

²King Abdulaziz City for Science and Technology, Riyadh, Saudi Arabia

³Department of Genomics Research, King Fahad Medical City and King Abdulaziz City for Science and Technology, Riyadh, Saudi Arabia

⁴Computational Bioscience Research Center, King Abdullah University of Science and Technology, Thuwal 23955-6900, Saudi Arabia

[†]These authors contributed equally to this work.

Abstract: The development of lateral flow immunoassay (LFIA) using three-dimensional (3D) printing and bioprinting technologies can enhance and accelerate the optimization process of the fabrication. Therefore, the main goal of this study is to investigate methods to speed up the developing process of a LFIA as a tool for community screening. To achieve this goal, an in-house developed robotic arm and microfluidic pumps were used to print the proteins during the development of the test. 3D printing technologies were used to design and print the housing unit for the testing strip. The proposed design was made by taking into consideration the environmental impact of this disposable medical device.

Keywords: Lateral flow immunoassay; COVID-19; Diagnostic tools; 3D Printing; Additive manufacturing technologies; Microfluidic pumps

*Correspondence to: Charlotte A. E. Hauser, Laboratory for Nanomedicine, Division of Biological and Environmental Science and Engineering, King Abdullah University of Science and Technology, Thuwal 23955-6900, Saudi Arabia; charlotte.hauser@kaust.edu.sa

Received: June 15, 2021; **Accepted:** July 29, 2021; **Published Online:** August 23, 2021

Citation: Alrashoudi AA, Albalawi HI, Aldoukhi AH, *et al.*, Fabrication of a Lateral Flow Assay for Rapid In-Field Detection of COVID-19 Antibodies Using Additive Manufacturing Printing Technologies. *Int J Bioprint*, 7(4):399. <http://doi.org/10.18063/ijb.v7i4.399>

1. Introduction

Severe acute respiratory syndrome coronavirus 2 (SARS-CoV-2) is the causative virus of coronavirus disease 2019 (COVID-19), and the first case was reported in China in December 2019^[1]. SARS-CoV-2 is a RNA virus that belongs to the coronavirus family and has multiple structural proteins on its surface, including spike, nucleocapsid, membrane, and envelope proteins^[2]. The virus causes severe respiratory symptoms requiring mechanical ventilation and intensive care unit admission, and contributes to high mortality rates^[3]. Moreover, the virus had high transmissibility between humans,

and for that, the World Health Organization declared COVID-19 as a pandemic on March 11, 2020^[4]. Since then, huge efforts to identify people with active infection of SARS-CoV-2 were implemented in order to stop the spread of the virus. Detecting individuals with active infection require polymerase chain reaction testing in nasal or throat swab samples, and the test results are used to identify and isolate positive cases so as to limit the transmission of the virus^[5]. Antibodies against the viral spike and nucleocapsid surface proteins are developed and can be detected in the serum of infected 14 days after the infection^[6]. Thus, testing serum or blood samples for antibodies against the viral surface proteins, especially

IgG, would provide information about people who had a history of prior infection and have recovered from the disease^[6]. Therefore, antibody testing has an important role in epidemiological assessment of community spread of the virus and to guide policy-makers when designing and introducing protective measures^[7].

A recent study by Dan *et al.* reported that people who recovered from COVID-19 have immunity lasting for 6-8 months after the infection in which IgG antibodies could be detected by serology testing^[8]. Screening for COVID-19 antibodies could provide valuable information about the level of immunity in the community. The screening can also be an important part in identifying who is immune and who is not when a majority of people return to work and transition to the new normal^[7]. Furthermore, the detection of antibodies against SARS-CoV-2 can be used as a tool to monitor immunity against SARS-CoV-2 acquired through vaccines, which can be done using laboratory-based immunoassays such as chemiluminescence and enzyme-linked immunosorbent assay, or rapid tests such as lateral flow immunoassay (LFIA)^[9]. Indeed, a cost-effective diagnostic tool would be beneficial for wide community screening. Rapid tests offer comparable outcomes to the laboratory-based tests and can be used when there is a need to identify people with immunity against the virus within a few minutes while having the advantages of being user-friendly, portable, and not requiring expensive instruments^[10].

A LFIA is a point-of-care diagnostic device that offers a rapid and inexpensive test that targets analytes in the samples by providing qualitative or semi-quantitative results^[11]. It consists of four essential parts, namely, the sample pad, conjugate pad, nitrocellulose membrane, and the absorption pad, which are assembled and placed in a housing cassette. One of the most predominant advantages of LFIA is the simplicity of the device as it can be used in the field without the need for any special equipment or sample processing. Moreover, since the beginning of the COVID-19 pandemic, there has been a tremendous effort to develop LFIA that can be used to detect viral antigens or serum antibodies for the identification of infected individuals or immune individuals, respectively^[12,13]. As more research is being conducted to optimize and develop more accurate tests, there is a need for a rapid method to prototype and construct these LFIA.

Technologies such as three-dimensional (3D) printing and bioprinting can be used as tools to aid in the development of LFIA where time is of the essence such as global pandemic^[14]. A material extrusion-based 3D bioprinting technique was utilized during the testing strip development where microfluidic pumps and a robotic arm were used to print different antibodies for screening. The microfluidic pump system was used to dispense the

capturing material on the nitrocellulose membrane as it offers an easier and efficient way to test multiple proteins. Furthermore, the robotic arms provide fine control of the nozzle when dispensing the material, while the pumps ensure consistent volume of the material to be dispensed on the nitrocellulose membrane to capture antibodies against SARS-COV-2.

Another component of the LFIA is the cassette used to house and protect the testing strip from damage. Since the LFIA test can be used to detect different types of analytes, billions of LFIA tests and cassettes are manufactured annually^[11]. Recently, there has been an increase in awareness regarding the environmental impact of medical devices, especially disposable devices^[15-17]. Thus, the environmental impact should be taken into consideration when designing medical devices to limit this negative impact^[16]. Since the LFIA cassette is made of polymers, it would be beneficial to consider how it can be designed in a way to decrease its environmental impact. Furthermore, using computer simulation for the 3D design, these iterations could be tested before the fabrication process. Furthermore, the simulation could be utilized to design and 3D print cassette with minimum polymeric material using different technologies.

In the past two decades, 3D printing technologies have been developed as essential prototyping techniques, industrially known as additive manufacturing technology, which are used as the primary prototyping technology in many applications today^[18]. 3D printing provides an accessible method for fabrication of a customized design solution in a rapid controlled manner. Due to its high utility, it has developed tremendously in many fields, from aeronautics to sustainability, as well as medicine^[19-21]. In this study, 3D printing was used to fabricate cassettes for rapid in-field assays. 3D printing technology provides the freedom to fabricate and prototype any designs in a standard laboratory setting, and saves the time and effort of many researchers. Overtime, different types of 3D technologies have been developed, including material extrusion 3D printing and vat photopolymerization 3D printing. These 3D technologies were used to prototype and print the housing unit.

During the pandemic, there has been a massive increase in the innovations and application of 3D printing technologies. 3D printing technologies offered a wide range of on-demand solutions during a time where supply chains were constrained. Some of the applications of 3D printing during COVID-19 pandemic include the production of medical devices, personal protective equipment, and other devices that aid in controlling the spread of the virus^[22]. With the evolutionary mutations of SARS-CoV-2 virus, we are facing new variants such as Delta variant^[23,24]. Since the virus is changing at a fast pace, we need to utilize technologies that allow us

to adapt to these changes and provide rapid solutions to protect our community.

The advantage of using 3D printing over the traditional methods, such as laser cutting, is that 3D printing offers a prototyping method to test multiple designs in short period of time. In addition, ease of accessibility to 3D printers makes them suitable for prototyping in a laboratory setting. Once the design is tested and finalized using 3D printing technology, it can be sent out for mass production.

Here, we developed a LFIA test using multiple technologies to efficiently optimize the testing strips. Bioprinting and 3D printing techniques were used during the development of a rapid test for the detection of antibodies against COVID-19. A material extrusion-based bioprinting setup utilizing a robotic arm was used during the construction of the strips to aid the dispensing of the capturing materials. In addition, an additive manufacturing technology was used to build a housing unit for the strip in a layer-by-layer manner using photopolymerization technique. The design of the cassette was modified as needed to adapt with the rapid changes in the testing strip during the optimization process. Using finite element analysis (FEA), we were able to simulate the physical strains on the designed cassette to determine its minimum thickness while ensuring the practicality of use and durability when conducting the test.

2. Materials and methods

2.1. Materials

Forty nanometers Gold NanoSpheres 2 mM citrate (OD=1) was purchased from nanohybrids. SARS-CoV-2 (2019-nCoV) Spike S1-His Recombinant Protein (HPLC-verified) (Cat. No.: 40591-V08H) and Normal Rabbit Control IgG (Cat. No.: CR1) were purchased from Sino Biological. SARS-CoV-2 Spike Protein (S-ECD/RBD) Monoclonal Antibody (bcb03) (Cat. No.: MA5-35950) and Goat Anti-Rabbit IgG (H+L) Superclonal Secondary Antibody (Cat. No.: A27033) were purchased from Fisher Scientific. Mouse monoclonal (JDC-10) Anti-Human IgG Fc (HRP) (Ab99759) was purchased from Abcam. 1×Phosphate-buffered saline (PBS), sucrose, TWEEN 20, and bovine serum albumin (BSA), potassium carbonate, and Tris buffer were purchased from Sigma-Aldrich. All chemicals were used as received, without purification or modification. Cellulose fiber sample pads, glass fiber conjugate pads, and high-flow nitrocellulose membrane were purchased from EMD Millipore Corporation. Sample pads, conjugate pads, and absorbent pads of different sizes were purchased from Ahlstrom-Munksjo. Backing cards KN-2211 were purchased from Kenosha. FormLabs Photopolymer Resin White (FLGPWH04) was purchased from FormLabs.

2.2. Conjugation of the gold nanoparticles

To conjugate the gold nanoparticles (AuNP) with S1 spike protein (40591-V08H, Fisher) and Rabbit antibody, as shown in **Figure 1A**, 1 ml of 1 OD AuNP solution was used and the pH was adjusted to 8.5-9 using potassium carbonate (K_2CO_3). The protein was added to the AuNP suspension at a ratio of protein solution: AuNP solution of 1:100 (v: v) with a final protein concentration of 10 $\mu\text{g}/\text{ml}$, and the suspension was incubated for 2 h while mixing. Then, 250 μl of 5% BSA in TRIS buffer was added and mixed for an additional 15 min. Afterward, 100 μl of 1% TWEEN 20 in TRIS buffer was added to the suspension and centrifuged for 10 min at $8000\times g$ and 4°C . The supernatant was removed, and the precipitate was resuspended in 1 ml of Tris buffer (pH 8.5) + 1% BSA + 1% TWEEN 20 and centrifuged as before. Finally, the precipitate was resuspended in 100 μl of Tris buffer (pH 8.5) + 1% BSA + 1% TWEEN 20 + 20% sucrose to achieve a conjugated AuNP concentration of 10 OD. The same process was used when conjugating the S1 spike protein and rabbit antibodies to the AuNP.

To confirm the conjugation of the protein to the gold nanoparticles, UV-Vis Spectrometer (PerkinElmer Lambda 1050) was used to compare the UV-Vis spectra of the conjugated AuNP with ligand-free AuNP. We assessed the red shift in peak absorbance between the conjugated AuNP and ligand-free AuNP which can be used to confirm the conjugation. The sample was scanned from 800 nm to 250 nm with a data interval of 1 nm and a scanning speed of 266.75 nm/min. To assess

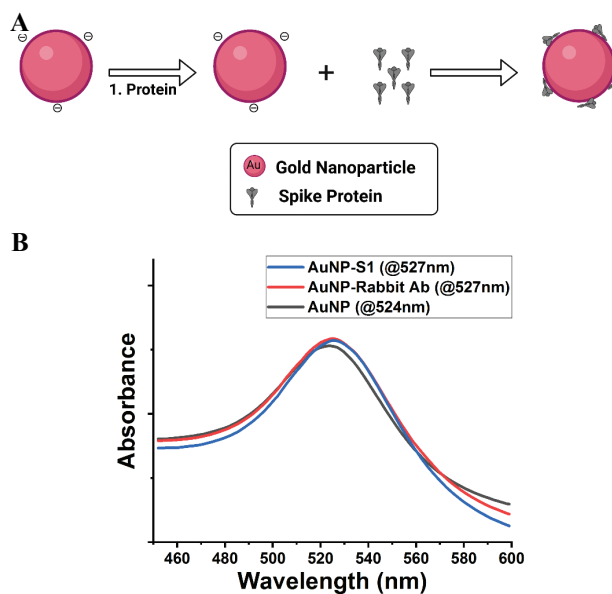


Figure 1. (A) Schematic representation of the physical conjugation process between the gold nanoparticles and the proteins of interest. (B) Detection of conjugated AuNP with antibodies and proteins by UV/VIS spectroscopy.

the attachment of the proteins to the gold nanoparticles, we performed UV–VIS absorption scan in which we compared AuNP-S1, AuNP-rabbit antibody conjugates to ligand-free AuNP. The conjugated nanoparticles showed a 3 nm shift compared to the ligand-free nanoparticles, as shown in **Figure 1B**, indicating the success of the functionalization of the 1 mL gold nanoparticles to the 10 µg of the S1 protein, and rabbit antibody^[25]. The red shift in peak absorbance is an indication of the enlargement of the gold nanoparticle size from the attachment of the proteins to the nanoparticle^[26].

2.3. Assembly of the strip

To assemble the strip, first, the high-flow nitrocellulose membrane was mounted on the backing cards. Dispensing of the antibodies to the nitrocellulose membrane was done using a setup consisting of a robotic arm (Dobot Magician, Dobot, China) and a microfluidic pump (ExiGo, Cellix, Ireland), as depicted in **Figure 2**; this setup could be considered as material extrusion-based bioprinting. Dispensing of the antibodies onto the nitrocellulose membrane was done using a 21 G needle attached to the robotic arm. The antibodies were dispensed at a rate of 200 µl/min and the robotic arm was programmed to move at a speed of 17 mm/s; antibodies were diluted in 1×PBS to be dispensed at a concentration of 200 µg/ml. These parameters ensured that antibodies were dispensed in a thick and continuous line. In particular, two antibody lines were printed on the nitrocellulose membrane. A test line was printed with anti-human antibodies (Abcam, Ab99759) and a control line was printed with anti-rabbit antibodies (Fisher, A27033). A video demonstrating the printing process is provided as the supplementary file. The strip was then dried at room temperature for 1 h. Then, the absorption pad was added to the backing card with a 2-3 mm overlap with the nitrocellulose membrane. Finally, the assembled backing card, nitrocellulose

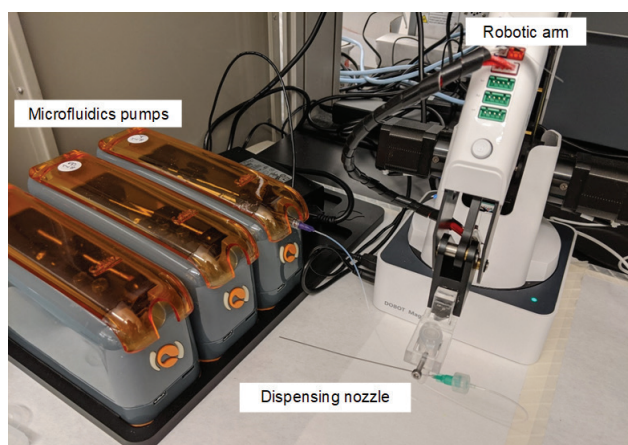


Figure 2. The printing setup consists of a robotic arm, microfluidics pumps, and dispensing nozzle.

membrane, and absorbent pad were cut into 5 mm wide strips.

2.4. Designing and 3D printing of the LFIA strip cassettes

NX computer-aided design (CAD) software was used in designing the housing units, along with SolidWorks as a supporting program. NX CAD was mainly used to design several iterations due to its capability in designing small features. NX CAD provided the simulation tools needed to test the assembly of the design before printing; the simulation of the designed structure was needed to design the locking mechanism as it requires a precise sizing to ensure proper locking after printing.

Multiple 3D printing technologies were used to ensure the design's maximum potential in prototyping these small housing units. Material extrusion 3D printing is the traditional 3D printing method, and vat photopolymerization 3D printing was used in prototyping the cassette designs. Using vat photopolymerization, 3D printing was about its ability to print a small housing unit with fine features in a short period of time. Furthermore, cassettes were printed with FormLabs white liquid resin and commercially available thermoplastic filament to keep the housing unit price reasonable. The vat photopolymerization 3D printer, FormLabs (Form 3), which was used in printing the housing unit, is capable of printing a hundred units a day.

We have devolved several design iterations to complement the rapid changes that we encounter during the test development. The first iteration of the designs started with mimicking the commercially available rapid tests^[27]. While modifying the test, the cassette design was modified as well leading to the final iteration design. Using different 3D printing technologies allowed us to try and change different features while developing the test.

2.5. FEA simulation for the final iteration of the cassette

LFIA test strips are usually single-use tests, and the housing units are there to protect the strip. Our aim during the designing process was to reduce the amount of material needed to build the cassette, thus reducing wasted and discarded material from each cassette used. FEA simulation was used to study the proposed design before printing to ensure that the design can sustain handling forces without breaking. The durability of the cassette is not essential in single-use devices; however, a minimum thickness for the proposed cassette is required to prevent it from breaking during the test and handling when polyethylene is used as a material for the designed cassette.

The FEA simulation was conducted using NX software. As NX was the CAD software used to design the

cassette, it was also used to perform the FEA simulation to ensure accurate simulation results for the proposed design. Furthermore, before FEA simulation, the two sides of the cassette were assembled without restricting the locking mechanisms to mimic the printing assembly. This setting gave a better understanding of the behavior of the dipsticks while exerting force (F). The type of element applied during this simulation was tetrahedral, with an element size equal to 1.43 mm. During the simulation, one side of the cassette was fixed, while the other side was the location of the applied force to the negative z-axis (Figure S1).

2.6. Testing of the assembled strip

The assembled strip was added to the cassette. A solution of AuNP-S1 and AuNP-rabbit antibody at a concentration of 10 OD was mixed together at a ratio of 1:1. The solution was then used by adding 10 μ l of the mixture into an Eppendorf tube, as shown in Figure 3. Afterward, a 1 μ l sample was added to the mixture and vortexed for 5 s. Here, we used SARS-CoV-2 Spike Protein Monoclonal Antibody (MA5-35950) at a concentration of 200 μ g/ml as a positive sample and 1 \times PBS was used as a negative sample. Then, the strip was submerged into the AuNP mixture until the strip fully absorbed the solution. Finally, it was submerged into another tube that contains 1 \times PBS as a running buffer to wash strips from any remaining particles.

3. Results and discussion

Here, we developed by assembling all the components a successful LFIA test that detects IgG antibodies. First, we conjugated SARS-CoV-2 spike protein to

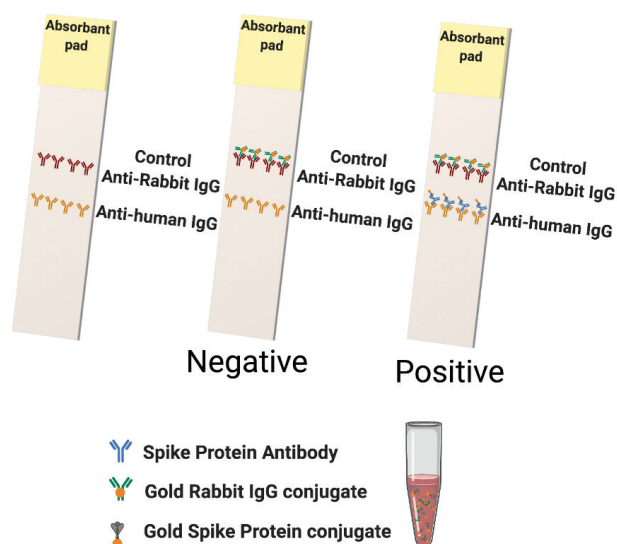


Figure 3. Illustration of an assembled dipstick test using the conjugated gold nanoparticles.

gold nanoparticles to capture SARS-CoV-2 antibodies in the sample tube. Then, the testing lines consisting of secondary antibodies were printed on the nitrocellulose membrane to capture primary antibodies, and the strip was placed in a 3D-printed housing cassette after careful design and strain simulation.

3.1. LFIA cassette designs and 3D printing

The housing unit design went through different iterations for adapting the changes and requirements for the test. These iterations were designed, fabricated, and assembled in the laboratory using specific requirements. The first two iterations are illustrated in the supplemental documents (Figures S2 and S3). These designs were made for testing using a full strip setup which includes the conjugate pad. Alternatively, the third iteration was a dipstick design which was made to house a strip that does not contain a conjugate pad. This provides a faster way to test the strip by removing an extra step that adds the conjugated AuNP to the conjugate pad.

In this study, we used two 3D printing technologies to print the proposed cassettes. Material extrusion 3D printing technology using thermoplastic filament was developed in the early 1990's^[28]. In the material extrusion 3D printing technique, a thermoplastic filament is fused using a mounted motor, which heats and melts the filament to be extruded during the printing process. On the other hand, vat photopolymerization technique uses a liquid photopolymer resin as a printing material, which is subjected to polymerization initiated by a projected laser. This process would selectively solidify the liquid resin against the platform, creating a 3D construct in a layer-by-layer fashion^[29]. The advantages of using vat photopolymerization over material extrusion 3D printing are the higher printing resolution and smoother finish surface^[30]. Table 1 provides a summary comparing the two 3D printing technologies. Figure 4 demonstrates a schematic of the process used to fabricate our cassettes using these two printing methods.

3.2. Dipstick housing unit

The dipstick housing unit design consists of a smaller unit with an opening from one side to be used for dipping the strip in the test solution as demonstrated in Figure 5A. This unit was engineered and designed by taking into consideration the security of the testing strip, as shown in Figure 5B. Since this design has a wide opening, it was essential to secure the strip, especially during the testing process. Therefore, a pressing locking mechanism was designed inside the housing unit, as shown in Figure 5C. Furthermore, the dipstick design was 3D printed using Form 3 printer (FormLabs) while taking into consideration the resolution of the used material.

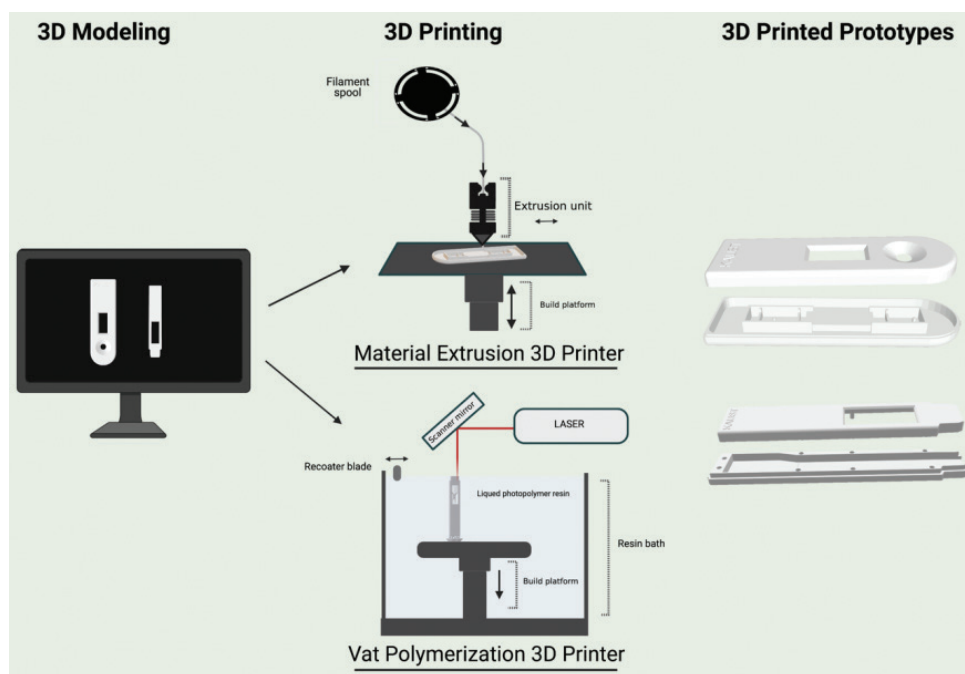


Figure 4. Schematic demonstration of the process used to fabricate the cassettes printed using material extrusion and vat polymerization 3D printing.

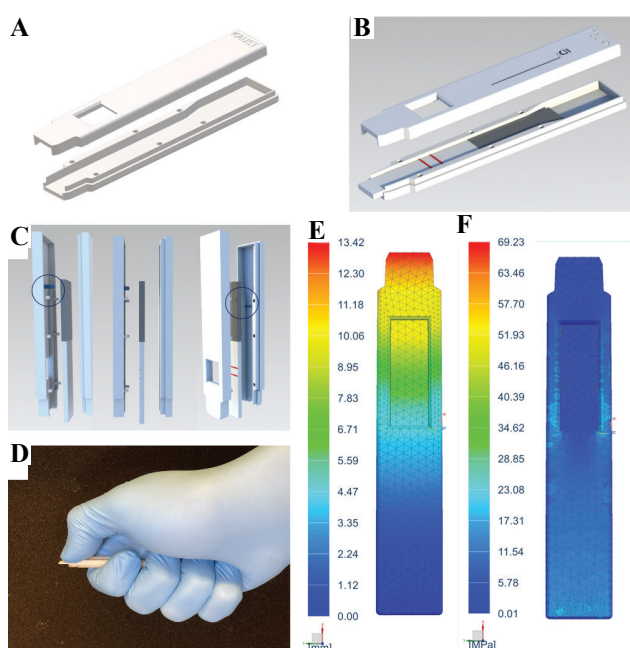


Figure 5. (A and B) CAD of the dipstick housing unit design. (C) CAD of the housing unit design with the bed pressing locking mechanism for securing the bed, the dipstick housing unit was 3D printed using vat photopolymerization. (D) The assumption and location of the applied force used in the simulation. (E) Simulation of the displacement for the dipstick cassette measured in mm when 5 N force was applied. (F) Simulation of the von Mises stress measured in MPa on the dipstick cassette when 5 N force was applied.

3.3. FEA simulation for the final iteration of the cassette

As the simulation was conducted on the same software, it made the process of changing and modifying the design more straightforward. During this experiment, we have changed the thickness of the dipstick several times to reduce the use of any unnecessary material in the printing process. We concluded that a cassette with thickness of 0.8 mm can be used and printed, and is the minimum thickness needed considering the simulation result.

The mass applied on the edge of the cassette during the simulation was set to be twice the normal handling force, where the normal handling force was assumed to be 2.5N. The assumption and location of the applied force were selected based on the actual state of a person applying pressure using one hand (**Figure 5D**). **Figure 5E** illustrates the dipstick cassette deformation for the pressing simulation. The maximum deformation value was observed to be 13.4 mm. Comparing the deformation result to the dimension of the model, the value range of the deformation is acceptable. **Figure 5F** illustrates the von Mises distribution of stress in the pressing simulation of the dipstick. From this result, it can be seen that the maximum stress of von Mises was 69.2 MPa. This is slightly lower than the yield strength of the material used in 3D printing which was approximately 70 MPa. Under these conditions, the results suggest that our dipstick design will tolerate the expected use.

Table 1. Summary of the differences between material extrusion and vat photopolymerization 3D printing technologies.

Additive manufacturing technologies	Materials	Speed	Average cost of materials (kg)	Printing resolution	Limitation
Material extrusion ^[31,32]	Plastic filaments (PLA, ABS, ASA, PETG, and nylon)	Fast	Affordable; \$40	Low	Support material
Vat polymerization ^[32,33]	Liquid photopolymers and resins	Slow	Average; \$100	High	Support material and post-curing required

PLA: Polylactic acid; ABS: Acrylonitrile butadiene styrene; ASA: Acrylonitrile styrene acrylate; PETG: Polyethylene terephthalate glycol

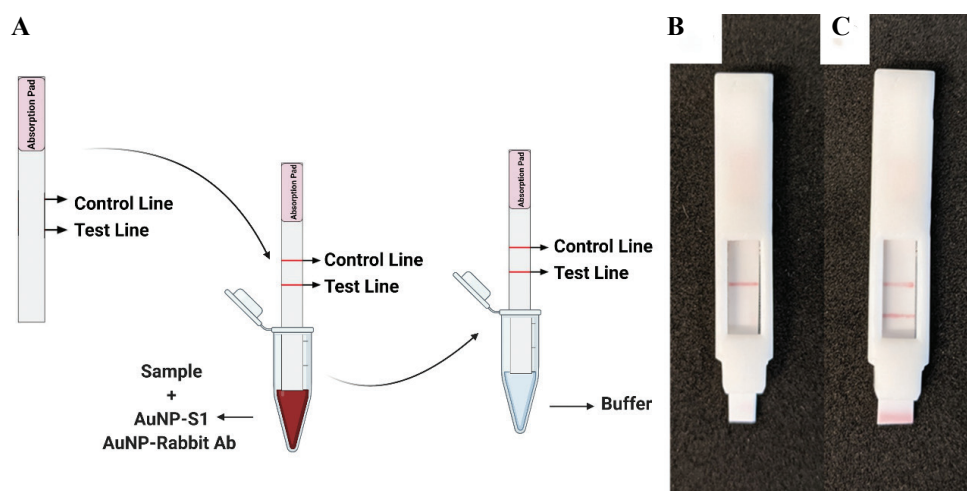


Figure 6. (A) Schematic of the dipping test without the housing cassette. (B) A lateral flow immunoassay (LFIA) showing a negative signal. (C) A LFIA showing a positive signal.

3.4. Testing of the assembled strip

LFIA dipstick strips were assembled to be tested with commercial SARS-CoV-2 antibodies to simulate positive or negative tests. **Figure 6A** shows a schematic of the test without the housing cassette. In this setup, if only the control line shows a red signal, then the sample is negative. If both control line and test line show a red signal, then the sample is positive. **Figures 6B** and **6C** depict two LFIA strips that were used as a dipstick in our testing. **Figure 6B** shows a negative sample in which a clear band is visible on the control line and no band is visible on the test line. On the other hand, **Figure 6C** demonstrates a positive sample containing anti-spike antibodies in which both the test and control lines are visible.

Using a dipstick design in prototyping, the LFIA provides a faster way to assess the test and ensure that all the test components are working as desired. When designing a new protein or modifying an existing one to enhance the sensitivity of the test, it is time-efficient to test the conjugated material using a dipstick LFIA before proceeding with further optimization processes to be used as a standard LFIA.

4. Conclusions

In this study, we demonstrated that the prototyping, printing, and assembly of an LFIA test are feasible

using an in-house developed setup. We showed that the test cassette could be prototyped to sustain mechanical stress applied to it by hand even if it was designed to be printed with minimum thickness to reduce material. To support the full functional capabilities of the device, we also demonstrated that bioprinting of the test lines with a robotic arm and microfluidic pump was accurate enough to detect IgG antibodies, when tested with protein-conjugated AuNP and commercially available antibodies.

Additive manufacturing technologies can be a great tool for prototyping and fabricating medical devices and diagnostics tools. These technologies can accelerate the optimization process by quickly adjusting to the designs and then 3D printing the device as needed. During the development phase of a new medical device and diagnostic tools, 3D printing can provide on-demand solutions despite the challenges.

Acknowledgments

This work was financially supported by King Abdullah University of Science and Technology (KAUST) and by King Abdulaziz City for Science and Technology (KACST) with a funded grant (4419-KACST COVID-19).

Conflicts of interest

The authors declare no conflict of interest.

Author contributions

C.A.E.H. proposed the research direction and guided the project. A.A.A., H.I.A., A.H.A. designed and performed the majority of the experimental parts. M.M., P.B. contributed to the experimental design and supervised the experimental work. A.A.A., H.I.A., A.H.A. wrote the manuscript. M.M. P.B. M.A. revised the manuscript. The authors have given approval to the final version of the manuscript.

References

- Guan WJ, Ni ZY, Hu Y, et al., 2020, Clinical Characteristics of Coronavirus Disease 2019 in China. *N Engl J Med*, 382:1708–20.
- Chan JF, Kok KH, Zhu Z, et al., 2020, Genomic Characterization of the 2019 Novel Human-pathogenic Coronavirus Isolated from a Patient with Atypical Pneumonia after Visiting Wuhan. *Emerg Microbes Infect*, 9:221–36. <https://doi.org/10.1080/22221751.2020.1719902>
- Huang C, Wang Y, Li X, et al., 2020, Clinical Features of Patients Infected with 2019 Novel Coronavirus in Wuhan, China. *Lancet*, 395:497–506.
- Cucinotta D, Vanelli M, 2020, WHO Declares COVID-19 a Pandemic. *Acta Biomed*, 91:157–60.
- Zou L, Ruan F, Huang M, et al., 2020, SARS-CoV-2 Viral Load in Upper Respiratory Specimens of Infected Patients. *N Engl J Med*, 382:1177–9. <https://doi.org/10.1056/nejmc2001737>
- To KK, Tsang OT, Leung WS, et al., 2020, Temporal Profiles of Viral Load in Posterior Oropharyngeal Saliva Samples and Serum Antibody Responses during Infection by SARS-CoV-2: An Observational Cohort Study. *Lancet Infect Dis*, 20:565–74. <https://doi.org/10.3410/f.737608898.793574123>
- Winter AK, Hegde ST, 2020, The Important Role of Serology for COVID-19 Control. *Lancet Infect Dis*, 20:758–59. [https://doi.org/10.1016/s1473-3099\(20\)30322-4](https://doi.org/10.1016/s1473-3099(20)30322-4)
- Dan JM, Mateus J, Kato Y, et al., 2021, Immunological Memory to SARS-CoV-2 Assessed for up to 8 Months after Infection. *Science*, 371:eabf4063. <https://doi.org/10.1126/science.abf4063>
- Martín J, Tena N, Asuero AG, 2021, Current State of Diagnostic, Screening and Surveillance Testing Methods for COVID-19 from an Analytical Chemistry Point of View. *Microchem J*, 167:106305. <https://doi.org/10.1016/j.microc.2021.106305>
- Schuler CF, Gherasim C, O’Shea K, et al., 2021, Accurate Point-of-care Serology Tests for COVID-19. *PLoS One*, 16:e0248729. <https://doi.org/10.1371/journal.pone.0248729>
- Banerjee R, Jaiswal A, 2018, Recent Advances in Nanoparticle-based Lateral Flow Immunoassay as a Point-of-care Diagnostic Tool for Infectious Agents and Diseases. *Analyst*, 143:1970–96. <https://doi.org/10.1039/c8an00307f>
- Adams E, Ainsworth M, Anand R, et al., 2020, Antibody Testing for COVID-19: A Report from the National COVID Scientific Advisory Panel. *Wellcome Open Res*, 5:139.
- Dinnes J, Deeks JJ, Berhane S, et al., 2021, Rapid, Point-of-care Antigen and Molecular-based Tests for Diagnosis of SARS-CoV-2 Infection. *Cochrane Database Syst Rev*, 3:CD013705. <https://doi.org/10.1002/14651858.cd013705>
- Ozolat IT, Hospodiuk M, 2016, Current Advances and Future Perspectives in Extrusion-based Bioprinting. *Biomaterials*, 76:321–43. <https://doi.org/10.1016/j.biomaterials.2015.10.076>
- Eckelman MJ, Sherman JD, 2018, Estimated Global Disease Burden From US Health Care Sector Greenhouse Gas Emissions. *Am J Public Health*, 108:S120–2. <https://doi.org/10.2105/ajph.2017.303846>
- Leiden A, Cerdas F, Noriega D, et al., 2020, Life Cycle Assessment of a Disposable and a Reusable Surgery Instrument Set for Spinal Fusion Surgeries. *Resour Conserv Recycl*, 156:104704. <https://doi.org/10.1016/j.resconrec.2020.104704>
- Unger SR, Hottle TA, Hobbs SR, et al., 2017, Do Single-use Medical Devices Containing Biopolymers Reduce the Environmental Impacts of Surgical Procedures Compared with their Plastic Equivalents? *J Health Serv Res Policy*, 22:218–25. <https://doi.org/10.1177/1355819617705683>
- Gebhardt A, 2011, Understanding Additive Manufacturing. In: Understanding Additive Manufacturing. Hanser Pub Inc., Cincinnati, OH. <https://doi.org/10.3139/9783446431621.fm>
- Joshi SC, Sheikh AA, 2015, 3D Printing in Aerospace and its Long-term Sustainability. *Virtual Phys Prototyp*, 10:175–85. <https://doi.org/10.1080/17452759.2015.1111519>
- Ng WL, Chua CK, Shen YF, 2019, Print Me An Organ! Why We Are Not There Yet. *Prog Polym Sci*, 97:101145.

- <https://doi.org/10.1016/j.progpolymsci.2019.101145>
21. Pant A, Lee AY, Karyappa R, *et al.*, 2021, 3D Food Printing of Fresh Vegetables Using Food Hydrocolloids for Dysphagic Patients. *Food Hydrocolloids*, 114:106546.
<https://doi.org/10.1016/j.foodhyd.2020.106546>
 22. Choong YY, Tan HW, Patel DC, *et al.*, 2020, The Global Rise of 3D Printing during the COVID-19 Pandemic. *Nat Rev Mater*, 5:637–9.
<https://doi.org/10.1038/s41578-020-00234-3>
 23. Harvey WT, Carabelli AM, Jackson B, *et al.*, 2021, SARS-CoV-2 Variants, Spike Mutations and Immune Escape. *Nat Rev Microbiol*, 19:409–24.
<https://doi.org/10.1038/s41579-021-00573-0>
 24. World Health Organization, 2021, Tracking SARS-CoV-2 Variants, World Health Organization, Geneva. Available from: <https://www.who.int/en/activities/tracking-SARS-CoV-2-variants>. [Last accessed on 2021 Jul 25].
<https://doi.org/10.12659/msm.933622>
 25. Jazayeri MH, Amani H, Pourfatollah AA, *et al.*, 2016, Enhanced Detection Sensitivity of Prostate-specific Antigen via PSA-Conjugated Gold Nanoparticles Based on Localized Surface Plasmon Resonance: GNP-coated Anti-PSA/LSPR as a Novel Approach for the Identification of Prostate Anomalies. *Cancer Gene Ther*, 23:365–9.
<https://doi.org/10.1038/cgt.2016.42>
 26. Pollitt MJ, Buckton G, Piper R, *et al.*, 2015, Measuring Antibody Coatings on Gold Nanoparticles by Optical Spectroscopy. *RSC Adv*, 5:24521–7.
<https://doi.org/10.1039/c4ra15661g>
 27. Yetisen AK, Akram MS, Lowe CR, 2013, Paper-based Microfluidic Point-of-care Diagnostic Devices. *Lab Chip*, 13:2210–51.
<https://doi.org/10.1039/c3lc50169h>
 28. Stansbury JW, Idacavage MJ, 2016, 3D Printing with Polymers: Challenges among Expanding Options and Opportunities. *Dent Mater*, 32:54–64.
<https://doi.org/10.1016/j.dental.2015.09.018>
 29. Infuehr R, Pucher N, Heller C, *et al.*, 2007, Functional Polymers by Two-photon 3D Lithography. *Appl Surface Sci*, 254:836–40.
<https://doi.org/10.1016/j.apsusc.2007.08.011>
 30. Milovanović A, Milošević M, Mladenović G, *et al.*, 2019, Experimental Dimensional Accuracy Analysis of Reformer Prototype Model Produced by FDM and SLA 3D Printing Technology. Springer International Publishing, Cham, p84–95.
https://doi.org/10.1007/978-3-319-99620-2_7
 31. Gibson I, Rosen D, Stucker B, *et al.*, 2021, Material Extrusion. In: Additive Manufacturing Technologies. Springer International Publishing, Cham, p171–201.
https://doi.org/10.1007/978-3-030-56127-7_6
 32. Kun K, 2016, Reconstruction and Development of a 3D Printer Using FDM Technology. *Proc Eng*, 149:203–211.
<https://doi.org/10.1016/j.proeng.2016.06.657>
 33. Gibson I, Rosen D, Stucker B, 2015, Vat Photopolymerization Processes. In: Additive Manufacturing Technologies: 3D Printing, Rapid Prototyping, and Direct Digital Manufacturing. Springer New York, p63–106.
https://doi.org/10.1007/978-1-4939-2113-3_4